

Multispectral Quantification of Tissue Types in a RIF-1 Tumor Model: Monitoring Response of a Single-Dose (1000cGy) Radiotherapy

E. C. Henning¹, C. Azuma², C. H. Sotak^{1,3}, K. G. Helmer¹

¹Department of Biomedical Engineering, Worcester Polytechnic Institute, Worcester, MA, United States, ²Department of Clinical Sciences, Tufts University School of Veterinary Medicine, North Grafton, MA, United States, ³Department of Radiology, University of Massachusetts Medical School, Worcester, MA, United States

Introduction

The development of MRI endpoints to detect an early tumor therapeutic response would aid greatly in patient management, opening the possibility for both rapid radio- and chemotherapeutic dose optimization and replacement of ineffective therapies with alternative treatment. Unfortunately, inter- and intra-tumor heterogeneity complicate the quantification of treatment response using MRI. A multi-spectral (MS) analysis approach in combination with ADC and T₂ maps has been shown to aid in the identification of multiple compartments within necrotic tissue.¹ Here we report on a single-dose radiotherapy study using RIF-1 tumors in which MS analysis, using k-means (KM) clustering, was used to identify multiple compartments in both viable and necrotic tissue. The goal is to identify sub-populations in each tissue type to better characterize tissue that includes heterogeneity.

Methods

Twenty-nine 6-8 week-old female C3H mice weighing 20-25g were anesthetized with an intraperitoneal injection of ketamine/xyzylazine (100mg/kg:10mg/kg). All mice were inoculated with 1×10⁶ RIF-1 cells (0.15ml), delivered through a subcutaneous injection into the right hind leg. Tumors were allowed to develop for 3-4 weeks, yielding an approximate 1.0cc starting volume.

Data for both control (n=16) and treatment (n=13) groups were acquired with a Bruker Biospin 2.0T/45 cm imaging spectrometer operating at 85.56 MHz for ¹H and equipped with ±20G/cm self-shielded gradients. The experiments involved multi-slice image acquisition along the coronal plane [128×128, FOV=3cm, slices=8, slice thickness=1mm]. A diffusion-weighted, spin-echo (SE) sequence was used to acquire the images at six b-values (b=50, 110, 210, 500, 690, 910 mm² s⁻¹) with diffusion sensitization applied along the read direction. Other acquisition parameters were: TR/TE=2000.0/53.0 msec, diffusion gradient duration δ=4.0msec, diffusion gradient separation Δ=35msec, resulting in an effective diffusion time t_{diff}=33.75msec. A T₂-weighted, SE sequence was used to acquire images at six echo times (TE = 12.2, 20, 35, 50, 65, 90 msec) with TR=2000msec. For the control group, tumors of varying volumes were imaged at a single time point and then extracted for histological examination. For the treatment group, tumors were irradiated with 1000cGy at a rate of 300cGy/min (Siemens Mevatron 77, 6 MeV electrons). Imaging was performed 1d pre-treatment, 5-hr, 1d-, 2d- post-treatment, and every 2d thereafter until tumor doubling (maximum 14d post-treatment).

Image reconstruction and ADC and T₂ parameter-map generation was performed using routines written in IDL[®] (RSI, Boulder, CO). Tissue classification was performed using the k-means (KM) clustering algorithm in a hierarchical manner. In the first step of the classification algorithm, it was applied to separate the data into two clusters (k = 2) of tumor tissue and background noise. All voxels classified as noise were set to zero and removed from further processing. In the second step, KM (k = 4) was applied to the remaining tissue voxels to segment the data into regions of viable tumor and necrosis. Average ADC and T₂ values were calculated for each cluster over all time points.

Results and Discussion

Fig. 1 shows the cluster assignments for a representative RIF-1 tumor. A central necrotic region is visible and is characterized by a small area of high ADC and high T₂-values surrounded by an area of somewhat lower ADC and T₂ values also associated with necrotic tissue. The viable tissue regions have similar T₂ values, but differing ADCs. The cluster with the higher ADC is adjacent to the necrotic clusters; the cluster with the lower ADC is located at the tumor periphery. The mean MR parameter values for each cluster in Fig. 1 are given in Table 1. Fig. 2 shows the temporal changes in individual cluster volume fractions (percent of total volume) pre- and post-irradiation for the treatment group. The total viable fraction decreased out to Day 4, with a concomitant increase in the total necrotic fraction. This decrease in viable fraction mirrors that of the initial decrease in tumor volume post-irradiation. Tumor volumes began to increase again after Day 4. Tumors that had not yet doubled in size by Day 10 were slower growing and had relatively smaller necrotic fractions. This accounts for suppression of the expected increase in necrotic fraction as the tumor regrows. In conclusion, this method allows the characterization of tissue heterogeneity within the broad categories of viable and necrotic tissue and may be used for tracking changes in tissue viability post-therapeutic intervention.

References

[1] Carano et al. *Proc. Int. Soc. Magn. Reson. Med.*, 490 (2002). [2] Duda RO and Hart PE. *Pattern Classification and Scene Analysis*. New York: John Wiley&Sons, 1973.

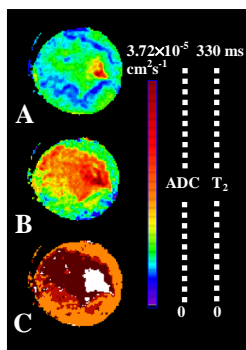


Fig. 1: A multispectral (MS) image of a representative RIF-1 tumor. (A) T₂ parameter map. (B) ADC parameter map. (C) KM map. The map derived by k-means (C) depicts the segmentation of the tumor into two regions of viable tumor and two regions of necrosis. Color assignments are: Viable 1 = Orange; Viable 2 = Red, Necrosis 1 = White; Necrosis 2 = Brown.

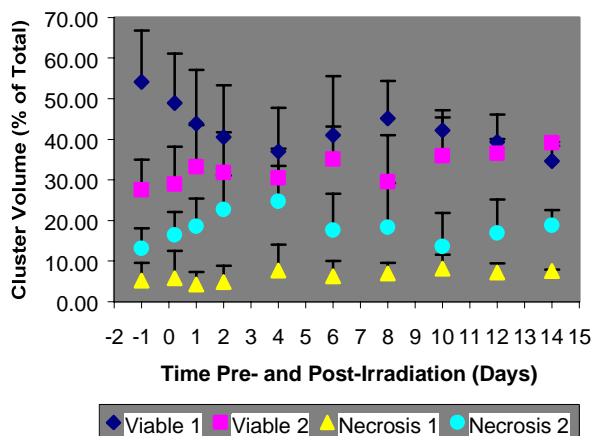


Fig. 2: Plot of the temporal evolution of individual cluster volumes for the treatment group.

Table 1: Mean parameters for the multispectral (MS) tissue classes of the RIF-1 tumor shown in Fig. 1. The measured parameters, ADC and T₂, are given as the mean ± standard deviation.

Tissue Cluster	ADC × 10 ⁵ (cm ² s ⁻¹)	T ₂ (ms)
Viable 1	0.9 ± 0.2	60 ± 10
Viable 2	1.4 ± 0.3	50 ± 9
Necrosis 1	1.7 ± 0.3	70 ± 10
Necrosis 2	2.3 ± 0.6	110 ± 50